International Journal of Computer Applications (0975 – 8887)
National Conference on Advancements in Alternate Energy Resources for Rural Applications (AERA-2015)

An Overview of Modelling and Control Strategies for FRT Conditions in DFIG based Wind Energy Systems

Sandeep Raikwal
Assistant Professor
Chandigarh University
Gharaun, Mohali

ABSTRACT

Wind energy systems based on doubly fed induction generators (DFIGs) have been dominantly used in high-power applications since they use power-electronic converters with ratings less than the rating of the wind turbine generators. The DFIG is very sensitive to unbalanced grid voltage as its stator is directly connected to the grid. The rotor and stator currents could be highly unbalanced even under a very small unbalanced grid voltage. So there is much more importance of designing and modelling of controllers for eliminating the fault and sustaining fault ride through condition. Modelling of controllers is different for steady state condition and transient conditions with fault ride through conditions.This paper presents an overview of trends and advancements in control strategies of DFIG based wind turbine system in transient conditions.

Keywords

DFIG,control strategies, DPC, DTC power quality, fault ride through ,VC

1. INTRODUCTION

Wind energy, recognized as the main contribution to low carbon societies, has become one of the subjects of much recent research and development globally. Recently, more and more modern wind turbines are being installed in distribution and rural grids with low X/R ratios, and in developing countries,where the distribution grids are quite weak. As a result, the application of wind generation systems based on modern power electronics has promoted the development of new functionalities for wind turbines, i.e., voltage or frequency regulation, islanding operation, and uninterruptable operation under nonideal gridvoltage conditions including symmetrical voltage dips, network unbalance, and harmonically distortions.

Among the various types of wind turbines, the variable speed wind turbines based on the doubly fed induction generator(DFIG), which have many advantages over the fixed speed induction generators or fully fed synchronous generators with full-sized converters, including variable-speed constant frequency(VSCF) operation, reduced flicker, independent control capabilities for active and reactive powers, and relatively lower converter cost and power losses, have attracted extraordinary attention by researchers and manufacturers all over the world.

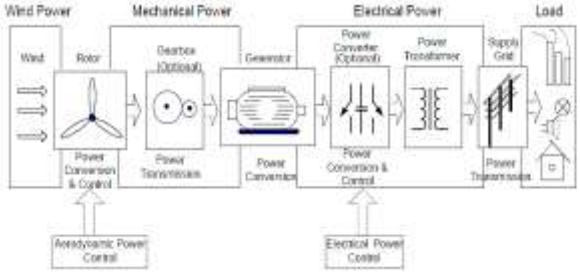

Fig 1: Complete Wind Energy Conversion system

Fig.1 represents the complete wind energy conversion systems (WECS), which converts the energy present in the moving air (wind) to electric energy. The power developed by the wind turbine mainly depends on the wind speed, swept area of the turbine blade, density of the air, rotational speed of the turbine and the type of connected electric machine. As shown in Fig.1, there are primarily two ways to control the WECS. The first is the Aerodynamic power control at either the Wind Turbine blade or nacelle, and the second is the electric power control at an interconnected apparatus, e.g., the power electronics converters. The flexibility achieved by these two control options facilitates extracting maximum power from the wind during low wind speeds and reducing the mechanical stress on the wind turbine during high wind speeds.

The aerodynamic wind power control is essentially intended to control the input power of the wind turbine. There are three ways to perform aerodynamic power control.

1. Pitch Control: The blades are physically rotated around their longitudinal axis.
2. Stall Control: The angle of the blade is fixed, but the aerodynamic performance of the design is such that at high wind speeds the blades stall.
3. Yaw Control: In this technique the entire nacelle is rotated around the tower to yaw (oscillate around a vertical axis) the rotor out of the wind. Due to its complexity and susceptibility to stress, this technique is not commonly used.

Currently, Pitch Control is the most common method for aerodynamic control. Almost all variable speed wind turbine topologies (including the DFIG) use Pitch Control. At wind speeds below the rated speed, it is used to maximize the energy capture. At wind speeds above the rated speed, it is used to reduce the mechanical stress on the system.

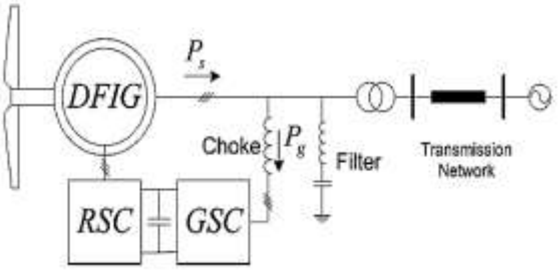

Fig.2: DFIG controller topology

DFIG is an induction machine with a wound rotor, where the rotor and stator are both connected to electrical sources. The rotor is fed with a back to back converter the AC-DC-AC. This template pro converter used on the rotor which consists of two voltage sourced converters i.e., rotor side converter (RSC) and grid side converter (GSC), between the components a dc-link. Capacitor is placed as energy storage. In order to keep the voltage variations (or ripple) in the dc-link voltage small With the rotor side converter it is possible to control the torque or the speed of DFIG and also the power factor at the stator terminals. The main objective for the GSC is to keep the dc link voltage constant regardless of the direction of rotor power. The RSC works at different frequencies, depending on the wind speed

2. RSC CONTROLLER TOPOLOGY

The RSC applies the voltage to the rotor windings of the DFIG. The purpose of the RSC is to control the rotor currents such that the rotor flux position optimally oriented with respect to stator flux in order that the desired torque is developed at the shaft. The RSC uses a torque controller to regulate the wind turbine output power and the voltage (or reactive power) measured at the machine stator terminals. The power is controlled in order to follow a pre-defined turbine power-speed characteristic to track the maximum power point. The actual electrical output power from the generator terminals, added to the total power losses (mechanical and electrical) is compared with reference power obtained from the wind turbine characteristic. Usually a proportional integral (PI) regulator is used at the outer control loop to reduce the power error (or rotor speed error) to zero. The q axis component controls the electromagnetic torque, $T_{e.}$

The grid usually requires the wind generator to have fault ride through capability during external AC fault. That means the generators are not allowed to disconnect from the network during disturbance such as voltage dip because of the relatively small rating of the RSC compared to generator rating it only provides partial control of the system. Therefore the overcurrent on the rotor side converter and subsequent over voltage on the RSC and subsequent over voltage on the converter DC link due to excessive power coming from the rotor side during network disturbance are easy to occur and become two main concerns of the system safety. Thus the main objective of the control system during network fault is to limit the rotor over current and DC over voltage

2.1 Gsc Controller Topology

The GSC aims to regulate the voltage of the DC bus capacitor. Moreover, it is allowed to generate or absorb reactive power for voltage support requirements the function is realized with two control loops as well: an outer regulation loop consisting of a dc voltage regulator. The output of the dc voltage regulator is the reference current I_{cd}^{ref} for the current regulator. The inner current regulation loop consists of a current regulator controlling the magnitude and phase of the voltage generated by converter from the I_{cd}^{ref} produced by the dc voltage regulator and specified q-axis I_{cq}^{ref}

3. VARIOUS CONTROL STRATEGIES

Modelling and control of DFIGs have been widely investigated based on well-established vector control schemes in a stator field-oriented frame of reference. The vector control is a fast method for independent control of the real/reactive power of a machine. Direct torque control (DTC) and direct power control schemes (DPC) have been presented as alternative methods which directly control machine flux and torque by selection of suitable vectors. In the following sections vector control, DTC and DPC are well explained for controlling of the grid side converter as well as rotor side converter the voltage and flux equations of a doubly fed induction machine are obtained from [5]

3.1 Vector Control Scheme

The standard voltage oriented vector control strategy is used for the machine side converter to implement control action. Here the real axis of the stator voltage is chosen as the d-axis [29]. The vector diagram is shown in Fig. 4.1. The mathematical modeling of the machine side converter is given in the following equations. Since the stator is connected to the utility grid and the influence of stator resistance is small, the stator magnetizing current i_m can be considered as constant. Under voltage orientation the relationship between the torque and the dq axis voltages, currents and fluxes can be written as follows. The stator flux Equations are written in Eq. (4.2) neglecting leakage inductances:

$$\left.\begin{aligned} \psi_{sd} &= 0 \\ \psi_{sq} &= L_s i_{sq} + L_m i_{rq} \\ &= (L_{ls} + L_m) i_{sq} + L_m i_{rq} \\ &= L_{ls} i_{qs} + (L_m i_{sq} + i_{rq}) \\ &\approx L_m i_m \end{aligned}\right\} (1)$$

The rotor voltage equation can be written by substituting the values of ψ_{rd} and ψ_{rq} as follows:

$$v_{rq} = R_r i_{rq} + \frac{d}{dt}\left(\frac{L_m^2}{L_s} i_m + \sigma L_r i_{qr}\right) + (\omega_e - \omega_r)\sigma L_r i_{rd} \quad (2)$$

On solving the above equation can be re written as:

$$v_{rq} = R_r i_{rq} + \frac{d i_{qr}}{dt}\sigma L_r + (\omega_e - \omega_r)\sigma L_r i_{rd} \qquad (3)$$

Similarly the simplified d-axis voltage is given by:

$$v_{rd} = R_r i_{rd} + \frac{d i_{dr}}{dt}\sigma L_r - (\omega_e - \omega_r)\left(\frac{L_m^2}{L_s} i_m + \sigma L_r i_{rq}\right) \quad (4)$$

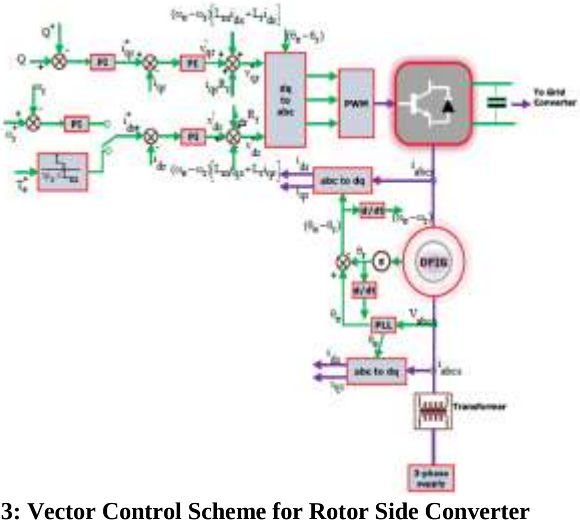

Fig.3: Vector Control Scheme for Rotor Side Converter

The unit vector is found in similar way as in the case of grid side converter. The reference value v_{rd}* and v_{rq}*which are being found from Eq. (3) and (4) are:

$$V_{rd}^{*} = V_{rd}^{'} + i_{rd}R_r - (\omega - \omega_r)[i_{qr}L_r + i_{qs}L_m] \qquad (5)$$

$$V_{rq}^{*} = V_{rq}^{'} + i_{rq}R_r - (\omega - \omega_r)[i_{dr}L_r + i_{ds}L_m] \qquad (6)$$

Where v'_{dr} and v'_{qr} are found from the current errors processing through standard PI controllers. The reference current i^*_{dr} can be found either from the reference torque given by Eq. (9) or form the speed errors (for the purpose of speed control) through standard PI controllers. Similarly i^*_{qr} is found from the reactive power errors. The reactive power and speed is controlled using the current control loops

The electromagnetic torque can be expressed as:

$$\tau_e = \frac{3}{2}\frac{p}{2}(\psi_{sd}i_{sq} - \psi_{sq}i_{sd}) \qquad (7)$$

The value of i_{rd}^* found using eq. (7) is:

$$i_{rd}^{*} = \frac{\tau_e \times L_s}{\psi_{sq} \times L_m} \qquad (8)$$

And reference torque value is given by:

$$\tau_e^{*} = \frac{P_m - P_{loss}}{\omega_r} \qquad (9)$$

The plant for the current loop is decided by the line resistance and reactance, whereas dc link capacitor is taken as the plant for the voltage loop. The plants for the current loop and the voltage loop are given in Eq. (10) and (11) respectively are:

$$F(s) = \frac{i_{rd}(s)}{v_{rd}^{'}(s)} = \frac{i_{rq}(s)}{v_{rq}^{'}(s)} = \frac{1}{\sigma L_r + R_r} \qquad (10)$$

$$G(s) = \frac{3PL_m}{4L_s\psi_{sq}(Js+B)} = \frac{K}{(Js+B)} \qquad (11)$$

The main objective of the grid side converter is to maintain dc-link voltage constant for the necessary action. The voltage oriented vector control technique is approached to solve this issue. The control scheme utilizes current control loops for i_d and i_q with the i_d demand being derived from the dc-link voltage error through a standard PI controller. The i_q demand determines the displacement factor on the grid side of the choke. The i_q demand is set to zero to ensure unit power factor. The control design uses two loops, i.e. inner current loop and outer voltage loop to provide necessary control action. The plant for the current loop is decided by the line resistance and reactance, whereas dc link capacitor is taken as the plant for the voltage loop. The plants for the current loop and the voltage loop are given in Eq. (12) and (13) respectively are:

$$F(s) = \frac{i_d(s)}{v_d^{'}(s)} = \frac{i_q(s)}{v_d^{'}(s)} = \frac{1}{L_s + R} \qquad (12)$$

$$G(s) = \frac{V_{dc}(s)}{i_d(s)} = \frac{3m_1}{2\sqrt{2}C_s} \qquad (13)$$

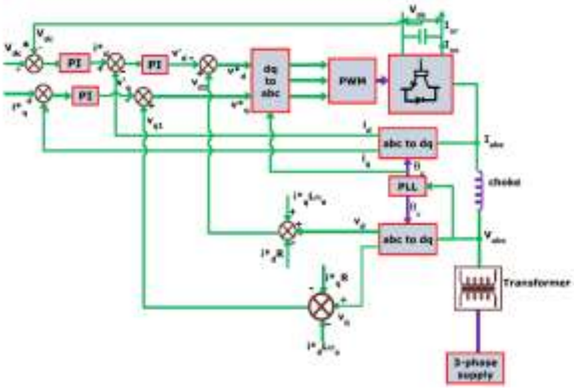

Fig.4: Vector Control Scheme for Grid Side Converter

The active and reactive power is controlled independently using the vector control strategy. Aligning the d-axis of the reference frame along the stator voltage position is found by Eq. (14), V_q= 0, since the amplitude of supply voltage is constant the active power and reactive power are controlled independently by means of id and i_q respectively following Eq. (15) are:

$$\tan\theta_e = \frac{v_q^s}{v_d^s} \qquad (14)$$

$$\left.\begin{aligned} P_s &= \frac{3}{2}(v_d i_d + v_q i_q) \\ Q_s &= \frac{3}{2}(v_d i_q - v_q i_d) \end{aligned}\right\} \qquad (15)$$

3.2 Direct Torque Control

The next generation of power control methods is direct torque control (DTC) [5], [6]. DTC decrease the use of machine parameters and reduces the complexity of vector control algorithms. The DTC method directly controls machine torque and flux by selecting voltage vectors from a look-up-table using the stator flux and torque information. One problem with the basic DTC scheme is that its performance deteriorates during starting and low-speed operations. Variable switching frequency and high torque ripple are the main limitations of hysteresis based DTC [33]. To address these limitations, DTC with space vector modulation based on synchronous reference frame transformation, predictive control and deadbeat control are reported here. A new DTC method where in rotor voltage vector is generated in polar form. Hence, the implementation of DTC using space vector modulation becomes simple compared to above mentioned methods. The method is also capable of independent control of torque and reactive power. The magnitude and angle of rotor voltage vector are controlled independently. The torque angle , is controlled in such a way that torque pulsations are reduced. To achieve this, a proportional-integral and resonant (PI+R) controller are used. The new DTC control method is a scalar control method, it does not require multiple reference frame transformation, sequential decomposition and notch filters to remove second harmonic components. The scheme of (PI+R) control in stationary frame is simple and complexity in calculations is significantly reduced.

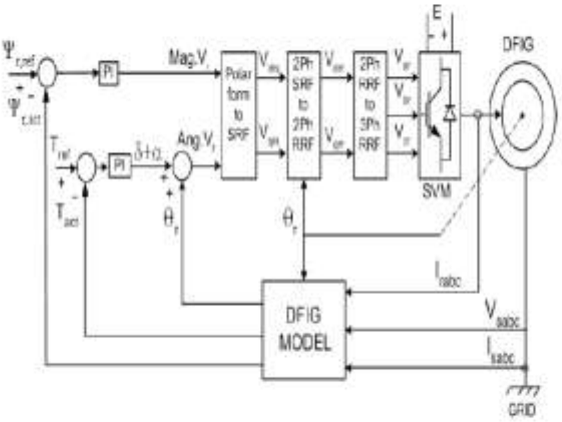

Fig 5: New Direct Torque Control method

Fig.5 shows the schematic representation of new DTC method. The torque developed by DFIG is also given by:

$$\tau_e = \frac{3}{2}\frac{P}{2}\frac{L_m}{L_r L_{se}}\psi_s \psi_r \sin\delta \qquad (16)$$

Where $L_{se} = L_s - \frac{L_m^2}{L_r}$ (17)

And δ is the angle between stator flux vector and rotor flux vector. Under balanced condition, the reference torque and actual torque are steady (dc) quantities. Single PI regulator is required to process the error between reference torque and actual torque. The output of PI regulator generates the signal proportional to (δ+α). Under unbalanced grid voltage condition, the stator flux vector consists of double frequency component which results in the oscillation of torque at this frequency. To eliminate the torque oscillation, it is required to modulate the rotor flux vector by controlling δ. Under unbalanced grid condition, the actual torque has an average dc value along with double frequency component. To process this double frequency fluctuating component of torque, the resonant regulator tuned at same frequency is used. PI regulator offers infinite gain for steady quantity, while resonant regulator offers an infinite gain at the selected resonant frequency. In addition, there is no phase shift and gain at other frequencies [36]. The block diagram of Proportional-integral and resonant (PI+R) controller is shown in Fig. 3. The output of PI regulator is a steady value of angle (δ+ α) which corresponds to steady error between reference torque and average value of actual torque. The output of resonant regulator is a double frequency component of torque angle. As a result, the proposed PI+R controller forces the steady state errors to be null for both steady and double frequency components of torque. The open loop transfer function (OLTF) of PI+R regulator is as follows:

$$OLTF = k_p + \frac{k_I}{s} + \frac{sk_R}{s^2+\omega_0^2} \qquad (19)$$

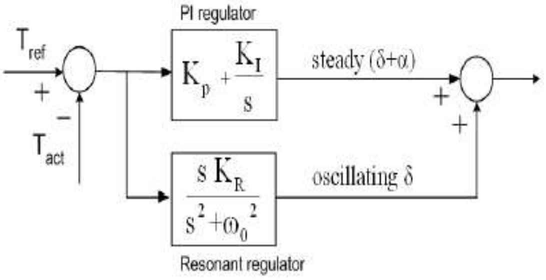

Fig 6: Block Diagram of Proportional Integral Resonant Controller

Where, K_R is the gain of resonant regulator, ω_0 is the tuned resonant frequency, which is selected as, double the supply frequency. It may be noted that a low value of K_R gives a very narrow frequency band. The block diagram for the implementation of proposed control scheme is shown in Fig. 4.Under unbalanced grid voltage condition, the grid side converter (GSC) maintains the dc link voltage constant.

3.3 Direct power control

Based on the principles of DTC strategy, direct power control (DPC) was developed for three-phase pulse width modulation (PWM) rectifiers [16]–[18]. From the previous researches it has been shown that DPC is a more efficient approach compared to modified DTC [26],[27], [28]. The main drawback of the vector control system is that its performance depends greatly on accurate machine parameters pertaining to the stator, rotor resistances, and inductances. Thus, the performance degrades when the actual machine parameters depart from the values used in the control system. Direct power control (DPC) abandons the rotor current control philosophy, which is the characteristic of FOC. Also, DPC achieves bang-bang active and reactive power control by the modulation of the rotor voltage in accordance with the active and reactive power errors. DPC is characterized by its fast dynamic response, simple structure and robust response against parameter variations. Converter switching states were selected from an optimal switching table based on instantaneous errors of active and reactive powers and the angular position of converter terminal voltage vector [16],[17], or virtual flux that is the integration of the converter output voltage[18]. More recently, DPC control of DFIG-based wind turbine systems has been proposed. Based on the principles of DTC strategy, direct power control (DPC) was developed for three-phase pulse width modulation (PWM) rectifiers [19]–[21]. Converter switching states were selected from an optimal switching table based on instantaneous errors of active and reactive powers and the angular position of converter terminal voltage vector [19],[20],or virtual flux that is the integration of the converter output voltage [21]. More recently, DPC control of DFIG-based wind turbine systems has been proposed [22], [23]. In [22], the control system was based on the estimated rotor flux. Switching vectors were selected from the optimal switching table using the estimated rotor flux position, and the errors of the rotor flux and the active power/torque. The rotor flux reference was calculated using the reactive power/ power factor reference. Since the rotor supply frequency, which equals the DFIG slip frequency, can become very low, rotor flux estimation is significantly affected by the machine parameter variations. In [23], a DPC strategy based on the estimated stator flux was proposed. Since the stator (network) voltage is relatively harmonic-free with fixed frequency, a DFIG's estimated stator flux accuracy can be guaranteed. Switching vectors were selected from the optimal switching table using the estimated stator flux position, and the errors of the active power and reactive powers. Thus, the control system is very simple, and the machine parameters' impact on system performance was found to be negligible. However a conventional DPC has switching frequency that varies significantly with active and reactive power variations, machine operating speed(rotor slip), and the power controllers' hysteresis bandwidth [22],[23]. In [24], the method predicts the DFIG's stator active and reactive power variations within a fixed sampling period, which is used to directly calculate the required rotor voltage to eliminate the power errors at the end of the following sampling period. This method directly controls the active power and the reactive power of the DFIM at constant switching frequency. Also, it has some privileges to the other DPCs; such as improvement of transient performance, negligible parameter effects on system performance and its good dynamic response. In this method the d-axis of the synchronous frame is fixed to the stator flux. As the stator is directly connected to the grid, and since the influence of the stator resistance can be neglected, the stator flux can be held constant. For a synchronous frame (the stator flux speed), the stator voltage vector is given as:

$$v_{sq} = \omega_e \psi_{sd} \qquad (20)$$

In [5] the stator current is expressed as:

$$I_{sdq}^{s} = \frac{L_r \psi_s - L_m \psi_r}{L_s L_r - L_m} = \frac{\psi_r}{L_{se} L_s} - \frac{L_m \psi_r}{L_{se} L_r} \qquad (21)$$

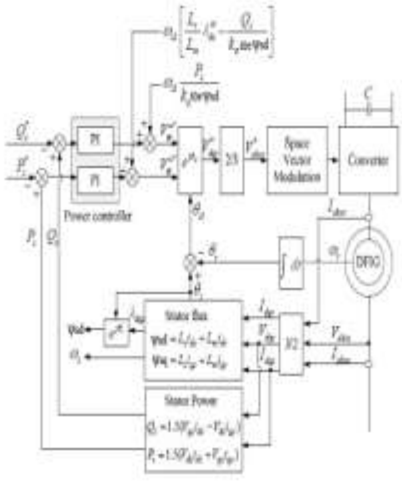

Fig.7: Schematic diagram of DPC

The stator active and reactive power inputs from the network can be calculated as:

$$P_s = -k_\sigma \omega_e \psi_{sd} \psi_{rq} \qquad (22)$$

$$Q_s = k_\sigma \omega_e \psi_{sd} \left(\frac{L_r}{L_m} \psi_{sd} - \psi_{rd}\right) \qquad (23)$$

$$k_\sigma = {}^{1.5 L_m}\!/_{(\sigma L_s L_r)}$$
(24)

As the stator flux remains constant, according to (22) & (23) the active and reactive power changes over a constant period of Ts are given by:

$$\Delta P_s = -k_\sigma \omega_e \psi_{sd} \Delta \psi_{rq} \qquad (25)$$

$$Q_s = -k_\sigma \omega_e \psi_{sd} \Delta \psi_{rd}) \qquad (26)$$

In the synchronous d-q reference frame, the rotor voltage is given by:

$$v_{rd} = r_r i_{rd} + j\omega_{sl} \psi_{rd} + \frac{d\psi_{rd}}{dt} \qquad (27)$$

$$v_{rq} = r_r i_{rq} + j\omega_{sl} \psi_{rq} + \frac{d\psi_{rq}}{dt} \qquad (28)$$

Combining equations (22) to (28) and neglecting the rotor resistance, the rotor voltage required to eliminate the power errors in the d-q reference frame is calculated as:

$$v_{rd} = \left(K_{PQ} + {}^{K_{IQ}}\!/_{s}\right)(Q_s - Q_s^*) + \omega_{sl} \frac{P_s}{k_\sigma \omega_e \psi_{sd}} \qquad (29)$$

$$v_{rd} = \left(KP + {}^{K_{Ip}}\!/_{s}\right)(P_s - P_s^*) + \omega_{sl} \left(\frac{L_r}{L_m} \psi_{sd} - \frac{Q_s}{k_\sigma \omega_e \psi_{sd}}\right) \qquad (30)$$

A schematic diagram of the DPC for a DFIG system is shown in Fig.7. The controller contains two PI controllers, one for an active power and one for reactive power, as well as a SVM unit. The stator active and reactive powers can be calculated directly. The stator flux is estimated using the measured stator voltages and currents in the stationary reference. Considering equations (21) - (30), a block diagram displays the dynamics existing between *Ps* and $V_{qr}{}^{*}$ on the one hand, and between *Qs* and $V_{dr}{}^{*}$on the other hand The overall control structure of a DPC is essentially constituted by one power controller. Fig. 4.6 shows that both dynamics are identical. Furthermore, this stator flux may be regarded as a constant disturbance whose effect on *Qs* can be removed easily simply by closing the reactive power control-loop via a compensator that includes an integral action. It is fundamental to note that the error signals feeding the PI controller are computed by subtracting the set-point of the variable to be controlled, Qs* or Ps*, from its actual value, Qs or Ps, respectively. This is due to the fact that Qs* and Qs are strictly negative. As a result, both Qs and Ps closed-loop dynamics can be represented by the following unique second-order transfer function:

$$\frac{P_s}{P_s^*} = \frac{Q_s}{Q_s^*} \approx \frac{K_{pp}\, k_\sigma \omega_e}{s^2 + k_{pp}\, k_\sigma \omega_e \psi_{sd}\, s + K_{IP}\, k_\sigma \omega_e}$$
(31)

From the transfer function (31), the dynamics are mainly influenced by constant *kσ* values that are determined via the stator and rotor leakage and the mutual inductance. Substituting the stator and rotor inductances, the parameter *kσ* is rewritten as follows:

$$k_\sigma = \frac{3}{2} \frac{1}{L_s L_r - L_m^2} \qquad (32)$$

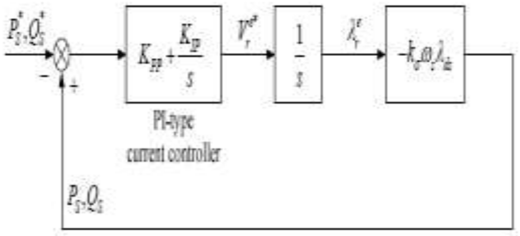

Fig.8: Overall Control System Of The DPC

4. CONCLUSION

In this paper dynamic modelling of DFIG using vector control, direct torque control and direct power control are discussed. It has been shown that DPC is a more efficient approach compared to modified DTC and VC.

5. REFERENCES

[1] R. Pena, J. C. Clare, G. M. Asher, "Doubly fed induction generator using back-to-back PWM converters and its application to variable speed wind energy generation," *IEE Proc. Elect. Power Appl.*, vol. 143, no. 3, pp. 231-241, 1996.

[2] S. Soter, R. Wegener, "Development of induction machines in wind power technology," *Proc. IEEE Int. Electric Mach. Drives Conf.*, vol. 2, pp. 1490-1495, 2007.

[3] W. Leonard, "Control of Electrical Drives," Springer, New York, 2001.

[4] N. Mohan, T. M. Undeland, W. P. Robbins, "*Power Electronics: Converters,* Applications and Design," Clarendon Press, Oxford, UK, 1989.

[5] P. Krause, O. Wasynczuk, S. Sudhoff, and I. P. E. Society, *Analysis of Electric Machinery and Drive Systems*. Piscataway, NJ: IEEE, 2002.

[6] G. A. Smith, K. Nigim, A. Smith, "Wind-energy recovery by a static Scherbius induction generator," *IEE Proc. C*, vol. 128, no.6, pp. 317-324, 1981.

[7] M. Mochmoum, R. Ledoeuff, F. M. Sargos, and M. Cherkaoui, "Steady state analysis of a doubly fed asynchronous machine supplied by a current controlled cyclo converter in the rotor," *IEE Proc. B*, vol. 139, no. 2, pp. 114-122 , 1992.

[8] F. Blaabjerg, R. Teodorescu, M. Liserre, A.V. Timbus, "Overview of Control and Grid Synchronization for Distributed Power Generation Systems," *IEEE Trans. Ind. Elect.*, vol. 53, no. 5, pp.1398-1409, 2006.

[9] R. Wu, S. B. Dewan, G. R. Slemon, "Analysis of an ac to dc voltage source converter using PWM with phase and amplitude control," *IEEE Trans. Ind. Elect.* vol. 27, no. 2, pp. 355-364, 1991.

[10]]O. S. Ebrahim, P.K. Jain, G. Nishith, "New Control Scheme for the Wind-Driven Doubly Fed Induction Generator under and Abnormal Grid Voltage Conditions," *J. Power. Electron.* vol. 8, no. 1, pp.10-22, 2008.

[11] O. Abdel-Baqi, A. Nasiri, "A Dynamic LVRT Solution for Doubly-Fed Induction Generators" *IEEE Trans. Power. Electron.* vol. 25, no. 1, pp.193-196, 2010.

[12] Y. Zhou, P. Bauer, J.A. Ferreira, J. Pierik, "Operation of Grid-Connected DFIG Under Unbalanced Grid Voltage Condition" *IEEE Trans. Energy Conversion*., vol. 24, no.1, pp.240-246, 2009.

[13] P. Rodriguez, A. Luna, R. Teodorescu, F.Iov, F. Blaabjerg, "Fault ride-through capability implementation in wind turbine converters using a decoupled double synchronous reference frame PLL," *Proc. Euro. Conf. Power Electron. Appl.*, pp.1-10, 2007.

[14] I. Takahashi and T.Noguchi, "A new quick-response and highefficiency control strategy of an induction motor," Inst. Elect. Eng.Trans. Ind. Appl., vol.22, no.5, pp.820–827, 1986.

[15] Depenbrock, "Direct self-control (DSC) of inverter-fed induction machine," IEEE Trans. Power Electron., vol.3, no.4, pp.420–429,Oct. 1988.

[16] T. Noguchi, H. Tomiki, S. Kondo, and I. Takahashi, "Direct power control of PWM converter without power-source voltage sensors," IEEE Trans.Ind. Appl., vol.34, no.3, pp.473– 479, May/Jun.1998.

[17] Lie Xu and Yi Wang, "Dynamic Modeling and Control of DFIG-Based Wind Turbines under Unbalanced Network Conditions," *IEEE Trans. On Power Systems*, vol. 22, no. 1, pp. 314-322, February 2007

[18] G. Escobar, A. M. Stankovic, J. M. Carrasco, E. Galvan, and R. Ortega,"Analysis and design of direct power control (DPC) for a three phase synchronous rectifier via output regulation subspaces, " IEEE Trans.Power Electron., vol.18, no.3, pp.823–830, May 2003.

[19] M. Malinowski, M. P. Kazmierkowski, S. Hansen, F. Blaabjerg, and G. D. Marques ,"Virtual-flux-based direct power control of three-phase PWM rectifiers," IEEE Trans.Ind.Appl., vol.37, no.4, pp.1019–1027,Jul./Aug.2001.

[20] T. Noguchi, H. Tomiki, S. Kondo, and I. Takahashi, "Direct power control of PWM converter without power-source voltage sensors," IEEE Trans. Ind. Appl., vol.34, no.3, pp.473–479, May/Jun.1998.

[21] G. Escobar, A. M. Stankovic, J. M. Carrasco, E. Galvan, and R. Ortega, "Analysis and design of direct power control (DPC) for a three phase synchronous rectifier via output regulation subspaces," IEEE Trans.Power Electron., vol.18, no.3, pp.823–830, May2003.

[22] M. Malinowski, M. P. Kazmierkowski, S. Hansen, F. Blaabjerg, and GD. Marques," Virtual-flux-based direct power control of three-phase PWM rectifiers," IEEE Trans. Ind. Appl., vol 37, no.4, pp.1019–1027,Jul./ Aug. 2001.

[23] K. P. Gokhale, D. W. Karraker, and S. J. Heikkila," Controller for a wound rotor slip ring induction machine," U. S. Patent 6448735 B1,Sep.2002.

[24] L. Xu and P. Cart Wright, "Direct active and reactive power control of DFIG for wind energy generation," IEEE Trans. Energy Convers.,vol.21, no.3, pp.750–758, Sep.2006.

[25] H. Akagi, Y. Kanazawa, and A. Nabae, "Generalized theory of the instantaneous reactive power in three-phase circuits," in Proc. Int. Power Electron. Conf., 1983, pp. 1375–1386.

[26] [26]D. Zhi, L. Xu, and B. Williams, "Model-based predictive direct power control of doubly fed induction generators," *IEEE Trans. Power Electron,* vol. 25, no. 2, pp. 341–351, Feb. 2010

[27] P. Zhou, W. Zhang, Y. He, and R. Zeng, "Improved direct power control of a grid-connected voltage source converter during network unbalance," *J. Zhejiang Univ.-Sci. C*, vol. 11,no. 10, pp. 817–823, 2010.

[28] J. Hu, H. Nian, B. Hu, Y. He, and Z. Zhu, "Direct active and reactive power regulation of DFIG using sliding-mode control approach," *IEEE Trans. Energy Convers.*, vol. 25, no. 4, pp. 1028–1039, Dec. 2010.

[29] Y. Lai and J. Chen, "A New Approach to Direct Torque Control of Induction Motor Drives for Constant Inverter SwitchingFrequency and Torque Ripple Reduction," *IEEE Trans. Energy Conversion*, vol. 16, no.03, pp. 220-227, Sept. 2001.

[30] The Central Electricity Authority, (Technical Standards for Connectivity to the Grid) Regulations, 2007, 2/X/STD (CONN)/GM/CEA, Feb. 2007.

[31] J. Rodriguez, J. Pontt, C. Silva, R. Huerta and H. Miranda, "Simple direct torque control of induction machine using space vector modulation, *"Electronics Letters*, vol. 40, no. 7, April 2004.

[32] Ruben Pena, Roberto Cardenas, Enrique Escobar, Jon Clare, Pat Wheeler, "Control strategy for a Doubly-Fed Induction Generator feeding an unbalanced grid or stand-alone load," *Electric Power Systems Research,* vol.79, issue 2, pp. 355-364, February 2009.

[33] Lie Xu and Yi Wang, “Dynamic Modelling and Control of DFIG-Based Wind Turbines under Unbalanced Network Conditions,” *IEEE Trans. On Power Systems*, vol. 22, no. 1, pp. 314-322, February 2007.

[34] Lie Xu , “Coordinated Control of DFIGs Rotor and Grid Side Converters During Network Unbalance,” *IEEE Trans. on Power Systems*, vol. 23, no.3, pp. 1041-1049, May 2008.

[35] Jiabing Hu, Yikang He, “Modeling and enhanced control of DFIG under unbalanced grid voltage conditions,” *Electric* Power Systems Research,vol. 79, issue 2, pp. 273-281, February 2009.

[36] R. Teodorescu, F. Blaabjerg, M. Liserre and P.C. Loh, “Proportional resonant controllers and filters for grid-connected voltage-source converters,” *IEEE Proc.-Electr. Power Appl.*, vol. 153, no. 5, pp. 750-762, September 2006.

[37] Andreas Petersson et al, “Modelling and Experimental Verification of Grid Interaction of a DFIG Wind Turbine,” *IEEE Trans. on Energy Conversion*, vol. 20, no. 4, pp. 878-886, Dec 2005.

[38] P. C. Krause, O. Wasynczuk, S. D. Sudhoff, “*Analysis of electric machinery and drive systems*” A John Wiley and Sons, UK, 2002

[39] M. Patel, Wind and Solar Power Systems: Design, Analysis, and Operation. Boca Raton, FL: CRC, 2006.

[40] K. Xie and R. Billinton, “Determination of the optimum capacity and type of wind turbine generators in a power system considering reliability and cost,” *IEEE Trans. Energy Convers.*, vol. 26, no. 1, pp.227–234, Mar. 2011.

[41] Esmaeil Rezaei, AhmadrezaTabesh, *Member, IEEE*, and Mohammad Ebrahimi, “Dynamic Model and Control of DFIG Wind Energy Systems Based on Power Transfer Matrix” IEEE TRANSACTIONS ON POWER DELIVERY, VOL. 27, NO. 3, JULY 2012

[42] T. Zhou and B. François, “Energy management and power control of a hybrid active wind generator for distributed power generation and grid integration,” *IEEE Trans. Ind. Electron.*, vol. 58, no. 1, pp. 95–104, Jan.2011.

[43] J. Hu, H. Nian, H. Xu, and Y. He, “Dynamic modelling and improved control of DFIG under distorted grid voltage conditions,” *IEEE Trans. Energy Convers.*, vol. 26, no. 1, pp. 163–175, Mar. 2011.[5] L. Fan, H. Yin, and Z. Miao, “On active/reactive power modulation of DFIG-based wind generation for inter area oscillation damping,” *IEEE Trans. Energy Convers.*, vol. 26, no. 2, pp. 513–521, Jun. 2011.

[44] S. Muller, M. Deicke, and R. De Doncker, “Doubly fed induction generator systems for wind turbines,” *IEEE Ind. Appl. Mag.*, vol. 8, no. 3,pp. 26–33, May/Jun. 2002.

[45] E. Tremblay, S. Atayde, and A. Chandra, “Comparative study of control strategies for the doubly fed induction generator in wind energy conversion systems: ADSP-based implementation approach,” *IEEE Trans. Sustain. Energy*, vol. 2, no. 3, pp. 288– 299, Jul. 2011.

[46] M. Mohseni, S. Islam, and M. Masoum, “Enhanced hysteresis- based current regulators in vector control of DFIG wind turbines,” *IEEE Trans. Power Electron.*, vol. 26, no. 1, pp. 223–234, Jan. 2011.